ARTHRITIS & RHEUMATOLOGY
Vol. 66, No. 1, January 2014, pp 152–162
DOI 10.1002/art.38225

An Essential Role of Caspase 1 in the Induction of Murine Lupus and Its Associated Vascular Damage

J. Michelle Kahlenberg,[1] Srilakshmi Yalavarthi,[1] Wenpu Zhao,[1] Jeffrey B. Hodgin,[1] Tamra J. Reed,[1] Noriko M. Tsuji,[2] and Mariana J. Kaplan[1]

Objective. **Systemic lupus erythematosus (SLE) is a systemic autoimmune syndrome associated with organ damage and an elevated risk of cardiovascular disease resulting from activation of both innate and adaptive immune pathways. Recently, increased activation of the inflammasome machinery in SLE has been described. Using the mouse model of pristane-induced lupus, we undertook this study to explore whether caspase 1, the central enzyme of the inflammasome, plays a role in the development of SLE and its associated vascular dysfunction.**

Methods. **Eight-week-old wild-type (WT) or caspase $1^{-/-}$ mice were injected intraperitoneally with phosphate buffered saline or pristane. Six months after injection, mice were euthanized, and the development of a lupus phenotype and vascular dysfunction was assessed.**

Results. **While WT mice exposed to pristane developed autoantibodies and a strong type I interferon response, mice lacking caspase 1 were significantly protected against these features as well as against pristane-induced vascular dysfunction. Further, the development of immune complex glomerulonephritis, which was prominent after pristane exposure in WT mice, was significantly abrogated in caspase $1^{-/-}$ mice.**

Conclusion. **These results indicate that caspase 1 is an essential component in the development of lupus and its associated vascular dysfunction and that it may play an important role in the cross-talk between environmental exposures and autoimmunity development, thus identifying a novel pathway for therapeutic targeting.**

Systemic lupus erythematosus (SLE) is a systemic autoimmune syndrome with severe clinical manifestations and enhanced mortality rates triggered by immune-mediated organ damage and a significant increase in cardiovascular (CV) risk due to premature atherosclerosis (1). An important contributor to development of both SLE and its associated increased CV risk is the up-regulation of type I interferon (IFN) responses, which influence both innate and adaptive immune processes and promote vascular damage (2–4).

Tetramethylpentadecane, commonly known as pristane, is a naturally occurring hydrocarbon oil that can induce chronic inflammation when introduced into the peritoneal cavity. Pristane injection is recognized as a robust model of lupus development, replicating numerous human manifestations, including autoantibody generation, arthritis, and severe glomerulonephritis (5). Further, the inflammatory response to pristane results in a strong up-regulation of type I IFNs through Toll-like receptor 7 (TLR-7) and IFN regulatory factor 5 (IRF-5) activation, contributing to a lupus-like phenotype (5,6). Indeed, lack of the type I IFN receptor results in limited TLR-7 expression, decreased autoantibody synthesis, and hampered recruitment of inflammatory monocytes ($Ly\text{-}6C^{high}$) due to decreased synthesis of the chemokine CCL2/monocyte chemoattractant protein 1 (MCP-1) (7,8). Thus, this model replicates many phenotypic and functional abnormalities of human SLE and has proven very useful in identifying putative pathogenic mecha-

Supported by grants to Dr. Kaplan from the Alliance for Lupus Research and the NIH (Public Health Service [PHS] grant HL-088419). Dr. Kahlenberg's work was supported by a Rheumatology Scientist Development Award from the Rheumatology Research Foundation. Dr. Hodgin's work was supported by the NIH (PHS grant K08-DK-088944).

[1]J. Michelle Kahlenberg, MD, PhD, Srilakshmi Yalavarthi, MS, Wenpu Zhao, MD, PhD, Jeffrey B. Hodgin, MD, PhD, Tamra J. Reed, BS, Mariana J. Kaplan, MD: University of Michigan, Ann Arbor; [2]Noriko M. Tsuji, PhD: National Institute of Advanced Industrial Science and Technology, Tsukuba, Japan.

Address correspondence to J. Michelle Kahlenberg, MD, PhD, or Mariana J. Kaplan, MD, Division of Rheumatology, Department of Internal Medicine, University of Michigan, 1150 West Medical Center Drive, 5520 MRSB1, Ann Arbor, MI 48109. E-mail: mkahlenb@med.umich.edu or makaplan@umich.edu.

Submitted for publication April 16, 2013; accepted in revised form October 3, 2013.

nisms and environmental triggers in this disease in a type I IFN–dependent system.

The inflammasome is a multimolecular complex consisting of platform molecules, scaffolds, and caspase 1, the enzyme responsible for processing of interleukin-1β (IL-1β) and IL-18 to their active forms (9). Activation of the inflammasome results from detection of environmental danger signals, including intracellular bacteria and cholesterol crystals (9). A role of the inflammasome in SLE pathogenesis and organ damage has been recently proposed. Activation of the NLRP3 inflammasome by neutrophil extracellular traps (NETs), chromatin structures released by neutrophils as a form of cell death termed "NETosis," and associated LL-37 is enhanced in lupus macrophages (10). Further, immune complexes formed by lupus-associated autoantigens (double-stranded DNA [dsDNA] and RNP) and their respective autoantibodies can activate the inflammasome machinery in monocytes (11,12). Similar activation of the inflammasome was described following exposure to IFNα in endothelial progenitor cells (EPCs) in human and murine SLE (4). Because these cells are considered key in promoting vascular repair following an insult to the endothelium, inflammasome activation in this system may promote the enhanced CV risk in patients with SLE (4). However, it remains unclear if the inflammasome or its components serve as crucial mediators of autoimmune responses and organ damage in vivo in SLE. Thus, we used the pristane-induced lupus model to examine whether the central enzyme of the inflammasome, caspase 1, was required for lupus development and severity.

MATERIALS AND METHODS

Mice. All animal protocols were reviewed and approved by the University of Michigan's committee on use and care of animals. Breeding pairs of caspase $1^{-/-}$ mice were initially obtained from Dr. R. A. Flavell (Yale University, New Haven, CT) and backcrossed onto the BALB/c background for at least 8 generations. Wild-type (WT) BALB/c and C57BL/6 mice were obtained from The Jackson Laboratory. Breeding pairs of caspase $1^{-/-}$ mice on a C57BL/6 background were obtained from Dr. Gabriel Nunez (University of Michigan, Ann Arbor, MI). Mice were bred at the University of Michigan. For lupus induction, 8-week-old mice were administered a single 0.5-ml intraperitoneal (IP) injection of phosphate buffered saline (PBS) (as a control) or pristane (Sigma-Aldrich) and were euthanized 6 months postinjection for the studies.

EPC quantification and assessment of differentiation. Bone marrow mononuclear cells were quantified by flow cytometry as previously described (2). Briefly, EPCs were defined as CD34+CD309+ cells in the lineage-negative (CD19–, CD3–, and CD45–) gate. This number was then extrapolated to calculate the percentage of EPCs in the live cell gate and is presented as the total number of EPCs/10^6 isolated bone marrow cells. The following antibodies were used: biotin-conjugated anti-CD19 (eBioscience), biotin-conjugated anti-CD3e (eBioscience), phycoerythrin (PE)–Cy5–conjugated anti-CD45 (BioLegend), fluorescein isothiocyanate (FITC)–conjugated anti-CD34 (eBioscience), allophycocyanin-conjugated anti-CD309 (eBioscience), and Pacific Blue–conjugated anti–annexin V (BioLegend). To detect anti-CD19 and anti-CD3e, a streptavidin–PE–Cy5–conjugated secondary antibody was used (BioLegend). Flow cytometry was performed using a CyAn ADP Analyzer (Beckman Coulter).

Assessment of the capacity of bone marrow–derived EPCs to differentiate into mature endothelial cells (ECs) was performed as previously described (4). Briefly, bone marrow mononuclear cells were plated onto fibronectin-coated plates (Becton Dickinson) at a density of 1×10^6 cells/cm^2 in EGM-2 BulletKit media (Lonza) supplemented with 5% heat-inactivated fetal bovine serum. After 7 days in culture, live cells were incubated for 3 hours with FITC-conjugated *Bandeiraea* (*Griffonia*) *simplicifolia* lectin 1 (Vector) and Texas Red–conjugated diacetylated low-density lipoprotein (Di-Ac-LDL; Biomedical Technologies). To assess EC morphology and expression of mature endothelial markers, cells were analyzed using fluorescence microscopy as described elsewhere (4). A total of 3 random fields of view were acquired for every triplicate well; images were analyzed using the CellC program (https://sites.google.com/site/cellsoftware/download) to quantify mature ECs, which were considered those that costained with *Bandeiraea* (*Griffonia*) *simplicifolia* lectin 1 and Ac-LDL.

Assessment of endothelium-dependent vasorelaxation. Assessment of endothelium-dependent vasorelaxation was performed as previously reported (13). Briefly, following euthanasia, thoracic aortas were excised and cleaned. The endothelium was left intact, and 2-mm aortic rings were mounted in a myograph system (Danish Myo Technology) and bathed with aerated (95% O_2/5% CO_2) physiologic salt solution. Aortic rings were set at 700 mg of passive tension, equilibrated for 1 hour, with buffer change every 20 minutes. The vessels were contracted twice with physiologic salt solution containing 100 m*M* potassium chloride prior to performing contraction/relaxation measurements. Cumulative concentrations of phenylephrine (10^{-9}–10^{-5} moles/liter) were added to the bath to establish a contraction concentration-response curve. A phenylephrine concentration corresponding to 80% of maximum was added, and contraction was allowed to reach a stable plateau. Endothelium-dependent relaxation was then assessed via graded addition of acetylcholine in a cumulative manner.

Characterization of autoantibodies and cytokine synthesis. Total serum IgG, anti-dsDNA, and anti-RNP antibody levels were quantified by enzyme-linked immunosorbent assay (ELISA) using commercially available kits (Alpha Diagnostic), following the manufacturer's protocols. Plasma cytokine and chemokine levels were quantified in undiluted plasma samples using a custom-designed Milliplex assay (EMD Millipore). IL-18 levels were measured via ELISA (eBioscience).

Proteinuria, renal histopathology, and immune complex deposition scoring. Urine samples were collected prior to euthanasia and were assessed for total protein with a Bradford

assay (Bio-Rad), for microalbumin using an Albuwell kit (Exocell), and for creatinine using a Creatinine Companion kit (Exocell). Ratios of total protein to creatinine and microalbumin to creatinine were calculated to estimate 24-hour urinary protein excretion.

For glomerular immune complex deposition, frozen sections were quantified for C3 and IgG deposition as previously described (13). Briefly, sections were stained with FITC-conjugated anti-C3 (ICL) and Cy3-conjugated anti-mouse IgG (Sigma) for 1 hour at 4°C. DNA was visualized using Hoechst (Invitrogen). Immune complexes were scored in a blinded manner by 2 independent observers (JMK, JBH). A score on a scale of 0–3 was assigned for both C3 and IgG deposition based on intensity of signal, and scores were multiplied by 2 if the staining diffusely involved the glomeruli. Six glomeruli per mouse were scored, and the averaged score for each component (IgG and C3) was added to create the composite score.

To score glomerular inflammation, paraffin-embedded cortical sections were sectioned at 3 μm thickness. Periodic acid–Schiff–stained sections were examined and graded by one of the authors (JBH) in a blinded manner following procedures previously described by us (13). Briefly, a semiquantitative scoring system was used to assess 2 different parameters of activity (mesangial hypercellularity and endocapillary cellular infiltrate), as follows: 0 = no involvement, 0.5 = minimal involvement (<10% of a section), 1 = mild involvement (10–30% of a section), 2 = moderate involvement (31–60% of a section), and 3 = severe involvement (>60% of a section). An activity index was generated by compiling these scores.

Real-time polymerase chain reaction (PCR). Total RNA was purified via TriPure (Roche) from 1×10^6 peritoneal cells, half of a homogenized spleen, or 1×10^6 bone marrow cells isolated on a Histopaque 1083 (Sigma) gradient. One microgram of RNA was transcribed into complementary DNA using oligo(dT) and Moloney murine leukemia virus (Invitrogen) using a MyCycler thermocycler (Bio-Rad).

The following transcripts and primers were used: for MCP-1, 5′-AGGTCCCTGTCATGCTTCTG-3′ (forward) and 5′-GGATCATCTTGCTGGTGAAT-3′ (reverse); for myxovirus (influenza virus) resistance protein 1, 5′-GATCCGACTTCACTTCCAGATGG-3′ (forward) and 5′-CATCTCAGTGGTAGTCAACCC-3′ (reverse); for IRF-7, 5′-TGCTGTTTGGAGACTGGCTAT-3′ (forward) and 5′-TCCAAGCTC-CCGGCTAAGT-3′ (reverse); for IFNγ-inducible protein 10, 5′-ATCATCCCTGCGAGCCTAT-3′ (forward) and 5′-ATTCTTGCTTCGGCAGTTAC-3′ (reverse); for IFN-stimulated gene 15 (ubiquitin-like modifier), 5′-CAGAAGCAGACTCCTTAATTC-3′ (forward) and 5′-AGACCTCATATATGTTGCTGTG-3′ (reverse); for IFNγ, 5′-AGCGGCTGACTGAACTCAGATTGTA-3′ (forward) and 5′-GTCACAGTTTTCAGCTGTATAGGG-3′ (reverse); for β-actin, 5′-TGGAATCCTGTGGCATCCTGAAAC-3′ (forward) and 5′-TAAAACGCAGCTCAGTAACAGTCCG-3′ (reverse); for IL-18, 5′-ACTGTACAACCGCAGTAATACGC-3′ (forward) and 5′-AGTGAACATTACAGATTTATCCC-3′ (reverse); for IL-1β, 5′-CCCTGCAGCTGGAGAGTGTGGA-3′ (forward) and 5′-CTGAGCGACCTGTCTTGGCCG-3′ (reverse); for caspase 1, 5′-GACTGGGACCCTCAAGTTTT-3′ (forward) and 5′-CCAGCAGCAACTTCATTTCT-3′ (reverse); and for NLRP3, 5′-ATGCTGCTTCGACATCTCCT-3′ (forward) and 5′-AACCAATGCGAGATCCTGAC-3′ (reverse).

An ABI Prism 7900HT instrument (Applied Biosystems) was used for quantitative real-time PCR analysis. Samples were normalized to β-actin, and the fold change was expressed as pristane-treated compared to PBS-treated samples.

Characterization of peritoneal inflammatory infiltrate. Peritoneal cells were collected by lavage after euthanasia. Washed cells were incubated with fluorochrome-labeled antibodies (anti-CD11b, anti-F4/80, anti-CD11c, anti-CD4, anti–annexin V, and anti-CD317/PDCA [BioLegend], anti–Ly-6G, anti–Ly-6C, and anti-CD3e [BD Biosciences], and anti-CD8a [eBioscience]) and analyzed by flow cytometry. Neutrophils were defined as Ly-6G+/CD11b+ in the F4/80– gate, plasmacytoid dendritic cells (PDCs) as CD11c+PDCA+ in the live cell gate, myeloid DCs as CD11c+PDCA– in the live cell gate, inflammatory monocytes as CD11b+Ly-6C^{high} in the Ly-6G– gate, and T cells as CD3e+CD4+ or CD3e+CD8+. The final data were expressed as the percentage of cells positive for the specific marker per 10^6 cells collected.

Characterization of NETs. Bone marrow neutrophils were isolated via Percoll gradient based on a previously published protocol (14). Cells (1.5×10^5) were adhered onto poly-L-lysine–coated coverslips at 37°C and then treated overnight with 40 n*M* phorbol myristate acetate (PMA). Cells were washed and stained with murine anti–neutrophil elastase (Abcam) and Hoechst. NETs were visualized via fluorescence microscopy and counted as previously described by our group (15). Total cell numbers were determined by the number of nuclei present per image, and numbers of NETs were determined by counting the number of elongated DNA structures costaining with murine anti–neutrophil elastase and Hoechst.

Statistical analysis. The D'Agostino and Pearson omnibus normality test was used to evaluate Gaussian distribution of the data. Analysis of statistical differences between the means of normally distributed data was evaluated by Student's unpaired *t*-test, and Welch's correction was added when variances were statistically significant as judged by an F test to compare variances. Non-normally distributed data were evaluated by a Mann-Whitney test. Linear regression analysis was used to correlate anti-dsDNA titers with renal inflammation, and composite histologic scoring was used to correlate IL-18 levels with renal inflammation.

RESULTS

Pristane exposure results in up-regulation of the inflammasome machinery. Elevated levels of IL-18 and caspase 1 associated with SLE have been described (4,16,17), and IL-1β levels are known to be increased in pristane-injected mice (18). In order to confirm these findings in the pristane-induced lupus model, real-time PCR was used to quantify transcripts from splenocytes isolated from BALB/c mice 6 months after IP pristane injection. As shown in Table 1, pristane robustly induced inflammasome-associated transcripts, and a trend toward elevated IL-18 and IL-1β transcript levels was seen in the spleens of WT mice injected with pristane, but not in the spleens of caspase $1^{-/-}$ mice injected with

Table 1. Fold change in levels of splenic inflammatory transcripts 6 months after pristane injection in WT and caspase $1^{-/-}$ mice*

	WT mice		Caspase $1^{-/-}$ mice	
Gene	Fold change	P†	Fold change	P†
NLRP3	19.70 ± 8.352	0.0020	−0.4845 ± 0.6457	0.6753
CASP1	4.964 ± 2.034	0.0456	–	–
Il1b	106.4 ± 71.77	0.1418	−43.40 ± 37.77	0.4351
Il18	404.8 ± 286.4	0.0813	−14.53 ± 6.682	0.3358

* Values are the mean ± SEM.
† Calculated by comparison of ΔC_t between phosphate buffered saline–treated mice (7 wild-type [WT] and 11 caspase $1^{-/-}$) and pristane-treated mice (13 WT and 23 caspase $1^{-/-}$).

pristane. This suggests that the pristane-induced lupus model replicates the alterations of the inflammasome described in human SLE in a caspase 1–dependent manner and that it is a relevant model for studying the effects of caspase 1 on lupus pathogenesis.

Inflammatory responses to pristane are intact in WT and caspase $1^{-/-}$ mice. As pristane-induced lupus depends on recruitment of inflammatory cells, particularly inflammatory monocytes (19,20), into the peritoneal cavity, we determined whether a lack of caspase 1 modified inflammatory cell recruitment following pristane exposure. As shown in Figure 1A, the inflammatory response following pristane injection was vigorous in both WT and caspase $1^{-/-}$ BALB/c mice. Further analysis showed no difference in PDC, myeloid DC, or inflammatory monocyte recruitment to the peritoneal cavity (Figure 1B). An enhanced recruitment of neutrophils was observed in caspase $1^{-/-}$ mice (Figure 1B). Further, no difference was noted between WT and caspase $1^{-/-}$ mice in the number or size of peritoneal lipogranulomas following pristane exposure (data not shown). These results indicate that lack of caspase 1 does not significantly alter the recruitment of inflammatory cells into the peritoneal cavity or change the formation of lipogranulomas, which are considered a nidus of chronic inflammatory mediators for disease development (5,21).

Absence of caspase 1 protects against the development of lupus autoantibodies. In order to determine whether lack of caspase 1 is protective in a lupus model,

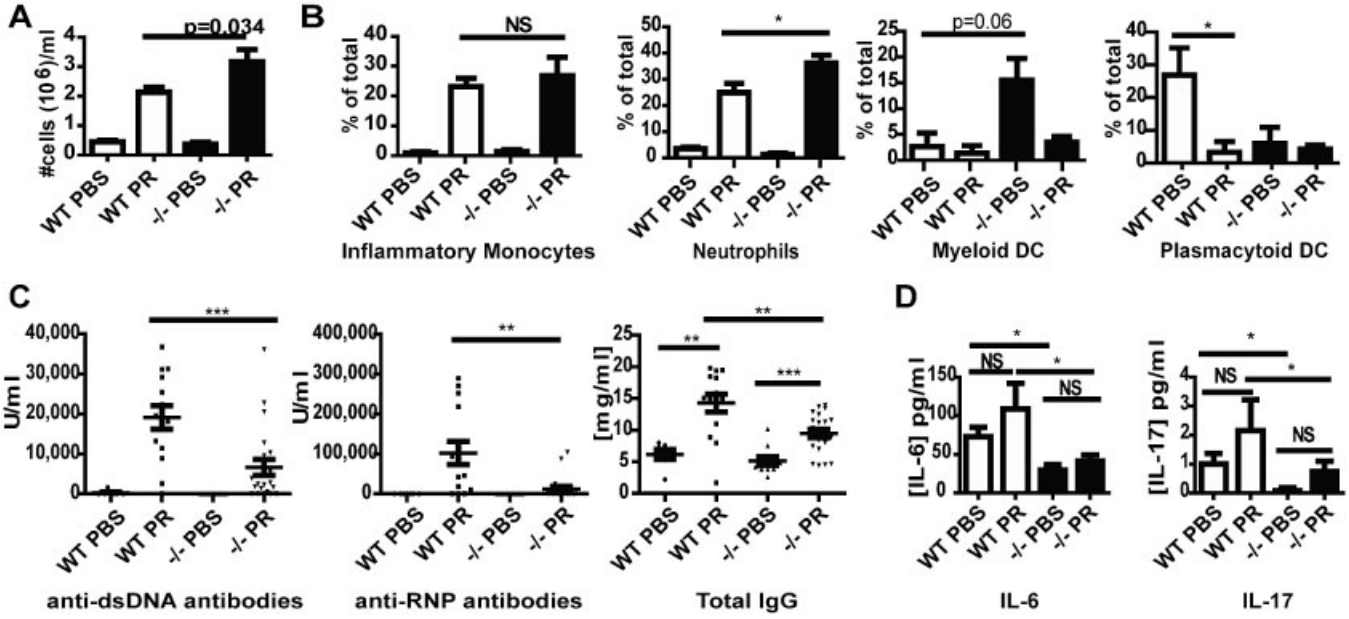

Figure 1. BALB/c caspase $1^{-/-}$ (–/–) mice have intact peritoneal inflammatory responses to pristane (PR) injection but display decreased autoantibody and inflammatory cytokine synthesis. **A** and **B,** Two weeks after pristane or phosphate buffered saline (PBS) injection, peritoneal fluid was harvested from wild-type (WT) mice (4 injected with PBS, 10 injected with pristane) and caspase $1^{-/-}$ mice (5 injected with PBS, 11 injected with pristane). Total cell numbers were counted and are plotted as the number of cells per ml of peritoneal fluid removed (**A**). Cell populations were quantified by flow cytometry and are expressed as a percentage of the total cell population when 1×10^6 total cells are examined (**B**). **C**, Antibody titers in sera from WT BALB/c mice or caspase $1^{-/-}$ BALB/c mice obtained 6 months after exposure to PBS or pristane were determined by enzyme-linked immunosorbent assay. Each symbol represents a single mouse. **D,** Plasma concentrations of interleukin-6 (IL-6) and IL-17 from mice described in **C** were quantified in undiluted samples using a custom-designed Milliplex assay. In **C** and **D,** there were 6 PBS-treated WT mice, 11 PBS-treated caspase $1^{-/-}$ mice, 13 pristane-treated WT mice, and 24 pristane-treated caspase $1^{-/-}$ mice. Bars show the mean ± SEM. $* = P < 0.05$; $** = P < 0.01$; $*** = P < 0.001$. NS = not significant; DC = dendritic cell; anti-dsDNA = anti–double-stranded DNA.

Table 2. Levels of plasma chemokines and cytokines in WT and caspase $1^{-/-}$ BALB/c mice 6 months after exposure to PBS or pristane*

Cytokine or chemokine	WT PBS-treated, pg/ml	WT pristane-treated, pg/ml	*P*, WT PBS-treated vs. WT pristane-treated	Caspase $1^{-/-}$ PBS-treated, pg/ml	Caspase $1^{-/-}$ pristane-treated, pg/ml	*P*, caspase $1^{-/-}$ PBS-treated vs. caspase $1^{-/-}$ pristane-treated	*P*, WT pristane-treated vs. caspase $1^{-/-}$ pristane-treated
MCP-1/CCL2	36 ± 10.37	174.8 ± 25.86	0.0024	78.36 ± 78.36	124.4 ± 16.1	0.0251	0.0856
MIP-1α/CCL3	9.5 ± 5.051	45 ± 10.57	0.0105	1.83 ± 1.273	14.23 ± 2.425	0.0004	0.0009
IP-10/CXCL10	205 ± 49.12	332.8 ± 29.11	0.0393	163.7 ± 25.16	335.8 ± 42.63	0.0007	NS
RANTES/CCL5	18.17 ± 5.474	18.92 ± 3.68	NS	51.09 ± 27.07	63.67 ± 25.35	NS	0.0371
GM-CSF	75.17 ± 18.4	85.00 ± 25.38	NS	53.40 ± 16.45	80.08 ± 25.13	NS	NS
IFNγ	0.6667 ± 0.494	0.6154 ± 0.368	NS	0.8000 ± 0.467	1.292 ± 0.682	NS	NS
IL-1β	9.000 ± 4.025	4.154 ± 2.189	NS	8.900 ± 3.761	3.167 ± 1.788	NS	NS
IL-2	26.83 ± 7.639	19.46 ± 8.883	NS	8.545 ± 4.137	7.875 ± 2.23	NS	NS
IL-4	0	0.7692 ± 0.077	NS	0	0	NS	NS
IL-5	4.5 ± 2.986	11.23 ± 3.327	NS	9.273 ± 4.083	6.833 ± 2.103	NS	NS
IL-10	0	0	NS	11.18 ± 11.18	11.79 ± 9.548	NS	NS
IL-12p40	27.33 ± 9.535	57.62 ± 42.07	NS	42.45 ± 11.89	80.21 ± 53.55	NS	NS
IL-12p70	5.333 ± 2.894	261.6 ± 229.8	NS	2.545 ± 1.065	11.13 ± 8.632	NS	NS
TNFα	2.5 ± 1.586	4.615 ± 1.357	NS	4.182 ± 1.536	3.25 ± 0.7	NS	NS

* There were 6 phosphate buffered saline (PBS)–treated wild-type (WT) mice, 11 PBS-treated caspase $1^{-/-}$ mice, 13 pristane-treated WT mice, and 24 pristane-treated caspase $1^{-/-}$ mice. Values are the mean ± SEM. MCP-1 = monocyte chemoattractant protein 1; MIP-1α = macrophage inflammatory protein 1α; IP-10 = interferon-γ–inducible protein 10; NS = not significant; GM-CSF = granulocyte–macrophage colony-stimulating factor; IFNγ = interferon-γ; IL-1β = interleukin-1β; TNFα = tumor necrosis factor α.

we examined whether autoantibody production was altered 6 months after pristane exposure in caspase $1^{-/-}$ mice compared to WT mice. As shown in Figure 1C, pristane induced a substantial increase in anti-dsDNA and anti-RNP antibodies in WT BALB/c mice 6 months postinjection. In contrast, autoantibody production in caspase $1^{-/-}$ mice was significantly blunted. Hypergammaglobulinemia, manifested by a rise in total IgG following exposure to pristane, was also decreased in caspase $1^{-/-}$ mice. Furthermore, levels of circulating inflammatory cytokines, such as IL-6 and IL-17, were lower in PBS- and pristane-treated caspase $1^{-/-}$ mice, suggesting an overall reduced inflammatory phenotype (Figure 1D). Unlike studies involving IRF-5–knockout mice (22), no differences in Th1 versus Th2 cytokine skewing were observed in WT mice compared to caspase $1^{-/-}$ mice following pristane exposure (Table 2). Overall, these results suggest that lack of caspase 1 modifies B cell responses and levels of proinflammatory cytokines and leads to decreased autoantibody formation in response to pristane.

Absence of caspase 1 decreases type I IFN signatures in pristane-induced lupus. Induction of a type I IFN response has been reported to play an important role in the development and severity of human and murine lupus (3,7,23,24). In the pristane-induced model of lupus, type I IFN pathways are required for disease development, as mice lacking the type I IFN receptor, TLR-7, or IRF-5 do not develop a clinical phenotype (6,7,20,25). Type I IFN responses were examined in the spleens and bone marrow of WT and caspase $1^{-/-}$ mice 2 weeks and 6 months after exposure to pristane. As shown in Figure 2A, 2 weeks after exposure to pristane, there were no significant differences in type I IFN responses between WT and caspase $1^{-/-}$ mice. In contrast, splenocytes and bone marrow cells isolated 6 months after treatment from WT mice, but not from caspase $1^{-/-}$ mice, displayed significant up-regulation of type I IFN–regulated genes when compared to littermates exposed to PBS. This repression of IFN signatures was not secondary to alterations in signaling through TLR-7, as exposure to the TLR-7 ligand R848 resulted in similar up-regulation of type I IFN–regulated genes in WT and caspase $1^{-/-}$ mice (Figure 2B).

Further, as an important role has been demonstrated for inflammatory monocytes in the initiation of type I IFN responses in the pristane-induced model of lupus (26), we examined whether differences in IFN signatures of these cells occurred in pristane-exposed WT and caspase $1^{-/-}$ mice. No significant differences were noted in the IFN signature of peritoneal inflammatory cells between WT and caspase $1^{-/-}$ mice 2 weeks after exposure to pristane (data not shown). These results indicate that lack of caspase 1 triggers repression of type I IFN signatures in pristane-treated mice.

The aberrant clearance of apoptotic debris in SLE may lead to autoantigen exposure and promotion of the type I IFN response and autoimmune pathways (27).

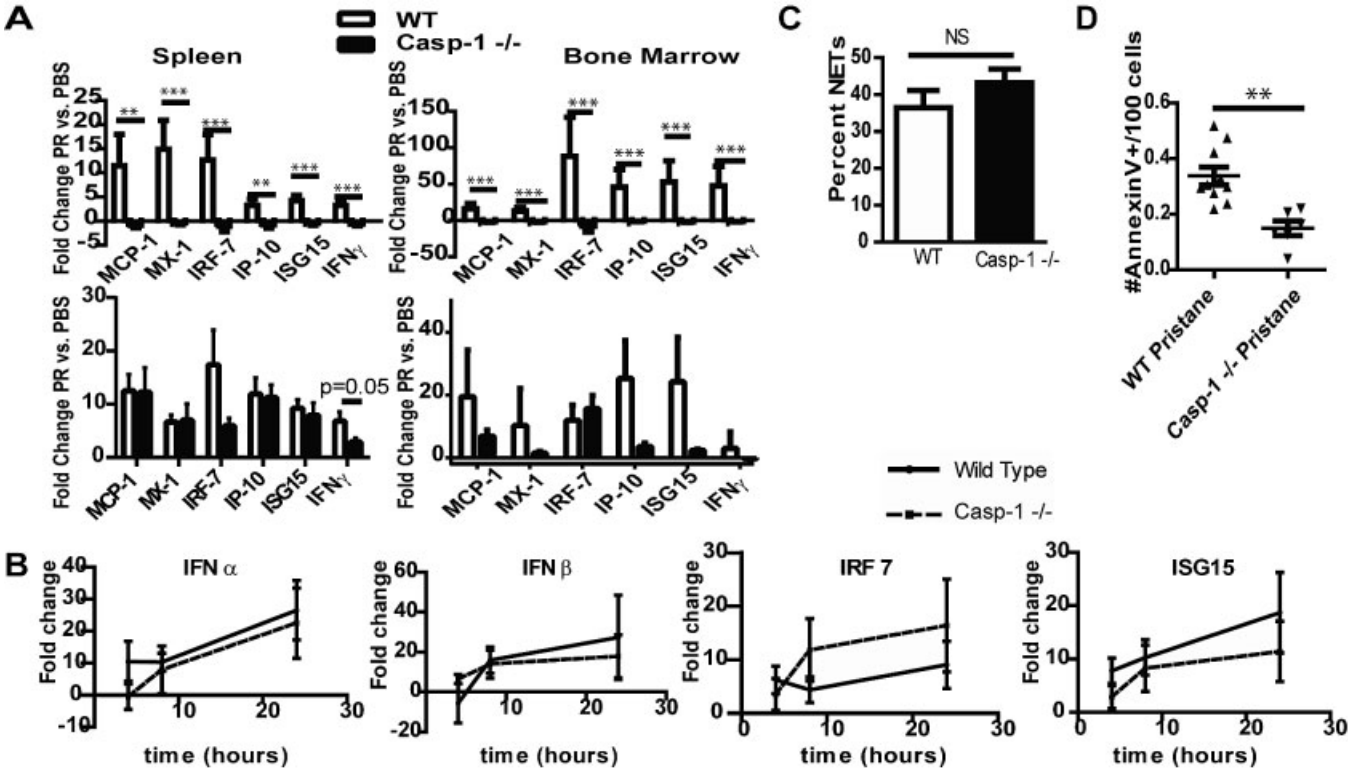

Figure 2. Type I interferon (IFN) signature induced after pristane exposure is abrogated in caspase $1^{-/-}$ (Casp-1 –/–) mice. **A,** Shown is the fold change in mRNA for type I IFN–regulated genes in splenocytes and bone marrow mononuclear cells isolated from BALB/c mice 6 months (top) or 2 weeks (bottom) after treatment. Following normalization to β-actin, comparisons of ΔC_t were made for pristane-treated versus PBS-treated mice. There were 7 PBS-treated WT mice, 11 PBS-treated caspase $1^{-/-}$ mice, 14 pristane-treated WT mice, and 24 pristane-treated caspase $1^{-/-}$ mice. **B,** Splenocytes from 10-week-old WT BALB/c mice or caspase $1^{-/-}$ BALB/c mice (n = 5 each) were stimulated with R848 for varying periods of time. Quantification of mRNA for type I IFN–regulated genes was performed as in **A**. **C,** Bone marrow neutrophils were isolated from WT or caspase $1^{-/-}$ mice (n = 4 each) and stimulated overnight with 40 n*M* phorbol myristate acetate. Neutrophil extracellular traps (NETs) were detected by extracellular colocalization of murine anti–neutrophil elastase and Hoechst. The percentage of NETs is calculated as number of NETting cells/total number of cells. **D,** Two weeks after pristane injection, peritoneal inflammatory cells were isolated, stained with annexin V, and analyzed via flow cytometry. Shown is the number of apoptotic/pyroptotic cells per 100 cells in the live cell gate for each mouse (10 WT mice, 6 caspase $1^{-/-}$ mice). Bars show the mean ± SEM. ** = $P < 0.01$; *** = $P < 0.001$. MCP-1 = monocyte chemoattractant protein 1; Mx-1 = myxovirus (influenza virus) resistance protein 1; IRF-7 = IFN regulatory factor 7; IP-10 = IFNγ-inducible protein 10; ISG-15 = IFN-stimulated gene 15 (see Figure 1 for other definitions).

Pristane exposure induces various forms of cell death, including NETosis in neutrophils and apoptosis in various inflammatory cells in the peritoneal cavity (18). Therefore, we examined whether the absence of caspase 1 modified cell death responses 2 weeks following pristane injection. We were unable to detect spontaneous NET formation in neutrophils isolated directly from the peritoneum after pristane exposure. In contrast, robust NET formation was observed following PMA stimulation of bone marrow–derived neutrophils from WT and caspase $1^{-/-}$ mice, suggesting that caspase 1 does not influence the NET response (Figure 2C).

In order to evaluate the role of caspase 1 in pristane-induced apoptosis and pyroptosis (inflammatory cell death), we used annexin V staining of peritoneal inflammatory cells isolated 2 weeks after pristane exposure. We detected a significant decrease in annexin V staining, which recognizes both apoptotic and pyroptotic cells (28), in peritoneal cells isolated from caspase $1^{-/-}$ mice when compared to WT mice (Figure 2D). This suggests that cell death following pristane exposure is abrogated in caspase $1^{-/-}$ mice. As aberrant cell death is considered an important phenomenon in modified autoantigen externalization, the formation of immune complexes, and the development of enhanced type I IFN responses (27), our observations suggest that caspase 1

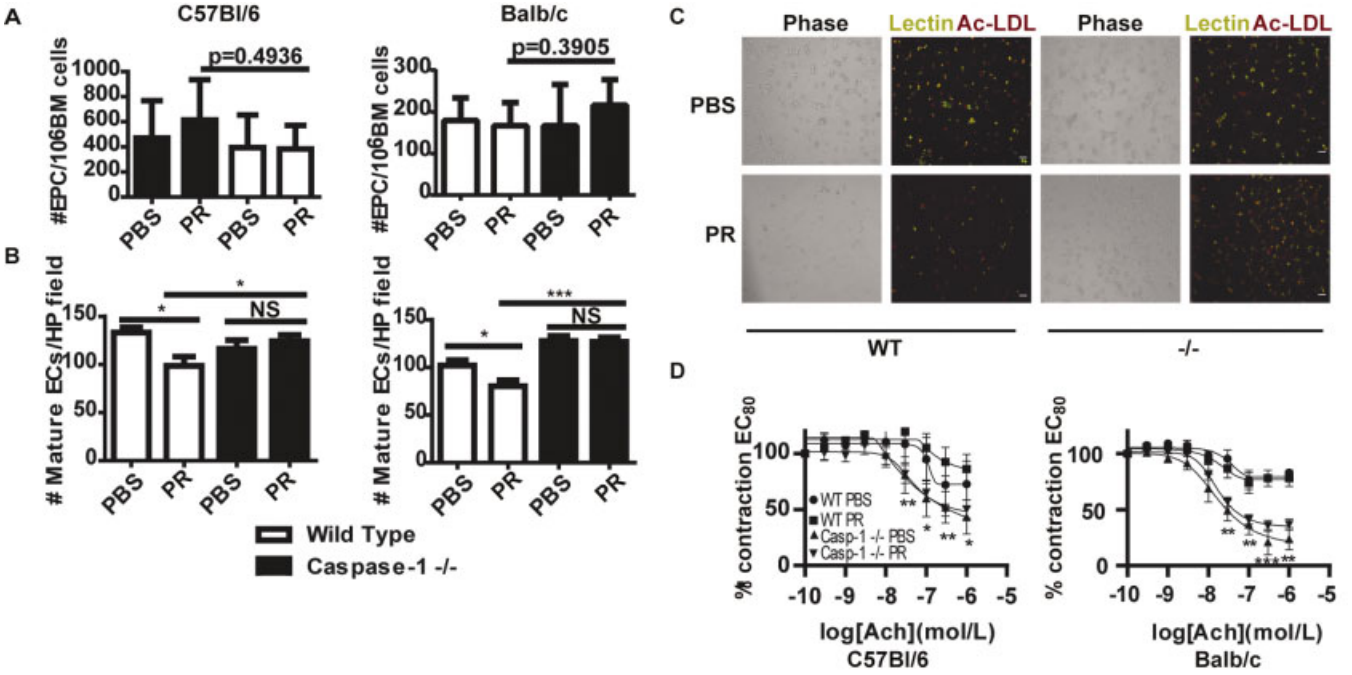

Figure 3. Increased endothelial progenitor cell (EPC) differentiation and endothelium-dependent vasorelaxation in the absence of caspase 1. **A,** Bone marrow (BM) was isolated from WT C57BL/6 mice or caspase $1^{-/-}$ (Casp-1 –/–) C57BL/6 mice (left) or from WT BALB/c mice or caspase $1^{-/-}$ BALB/c mice (right), and EPCs were quantified by flow cytometry. Results are the number of EPCs/10^6 BM cells for each group. **B,** BM cells were plated under proangiogenic conditions. After 7 days, the number of mature endothelial cells (ECs)/high-power (HP) field was quantified by fluorescence microscopy. Left, WT C57BL/6 mice compared to caspase $1^{-/-}$ C57BL/6 mice. Right, WT BALB/c mice compared to caspase $1^{-/-}$ BALB/c mice. $* = P < 0.05$; $*** = P < 0.001$. In **A** and **B,** 5 WT C57BL/6 mice were injected with PBS and 8 were injected with pristane, 10 caspase $1^{-/-}$ C57BL/6 mice were injected with PBS and 14 were injected with pristane, 7 WT BALB/c mice were injected with PBS and 14 were injected with pristane, and 11 caspase $1^{-/-}$ BALB/c mice were injected with PBS and 24 were injected with pristane. **C,** Shown are representative photomicrographs of the EC cultures from BALB/c mice depicted in **B**. Bars = 20 μm. **D,** Endothelium-dependent vasorelaxation of aortic rings was quantified following exposure of 80% contracted aortic rings to graded concentrations of acetylcholine (ACh). $* = P < 0.05$; $** = P < 0.01$; $*** = P < 0.001$ versus WT mice. Bars show the mean ± SEM. Phase = phase contrast; Ac-LDL = acetylated low-density lipoprotein; EC_{80} = effective concentration of phenylephrine for 80% maximal contraction (see Figure 1 for other definitions).

may play an important role in regulating type I IFN synthesis by modulating cell death pathways.

Absence of caspase 1 decreases markers of CV risk. The inflammasome has been implicated in inflammatory responses in atherosclerotic plaques (29), and lack of caspase 1 modulates severity of atheroma in murine models (30). We previously demonstrated that in vitro inhibition of caspase 1 improves the differentiation of human lupus EPCs into mature ECs, a phenomenon that may be important in preventing vascular damage in this disease (4,31,32). Thus, we examined whether lack of caspase 1 modified CV parameters in the pristane-induced model of lupus. Mice in both the BALB/c and C57BL/6 backgrounds were studied, as lupus models of various backgrounds display endothelial dysfunction to varying degrees (33).

Neither exposure to pristane nor absence of caspase 1 altered the number of bone marrow EPCs, as assessed by flow cytometry (Figure 3A). However, absence of caspase 1 significantly abrogated the inhibitory effects on EPC differentiation induced by pristane (Figures 3B and C). These observations confirm previous in vitro findings in human samples and indicate that caspase 1 is operational in vivo with regard to lupus-mediated EPC dysfunction. Previously, investigators in our group also showed that other murine models of lupus display impaired endothelium-dependent vasorelaxation, a phenomenon associated with progression to atherosclerosis in human systems (33). In pristane-treated C57BL/6 mice, but not in pristane-treated BALB/c mice, a similar decrease in endothelium-dependent vasorelaxation was observed following expo-

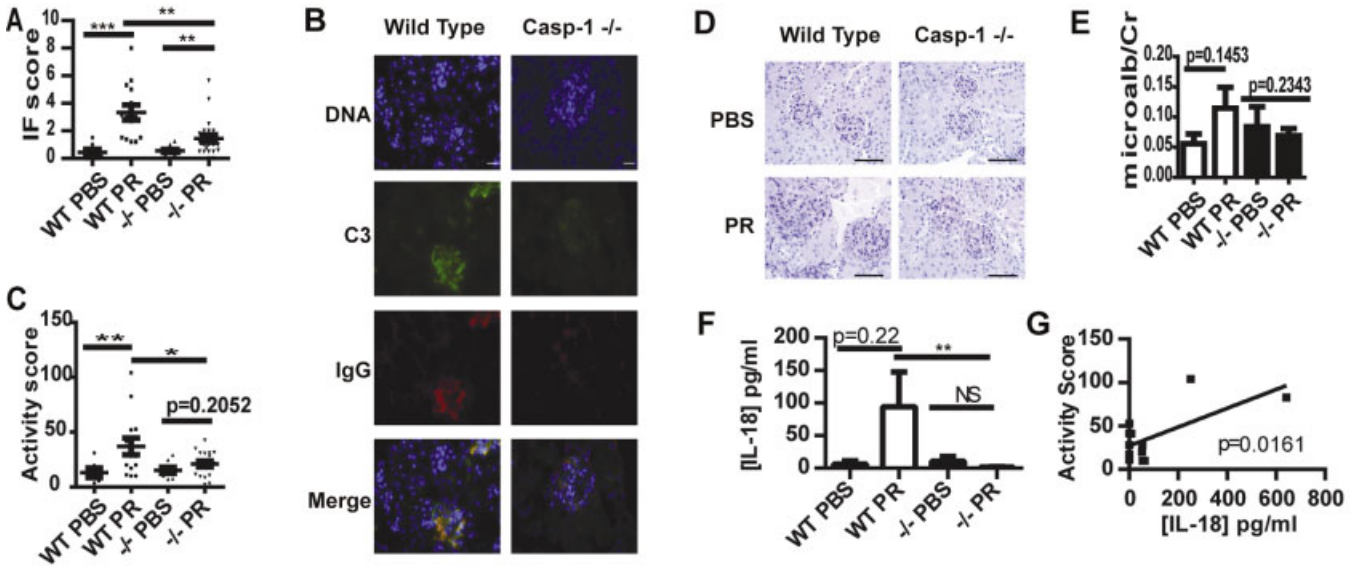

Figure 4. Caspase 1 modulates immune complex deposition and glomerular activity scores in lupus-prone mice. **A** and **B,** Deposition of C3 (green) and IgG (red) was quantified in kidneys obtained from WT BALB/c mice or caspase $1^{-/-}$ (Casp-1 –/–) BALB/c mice following exposure to PBS or pristane. Composite scores were averaged (**A**), and representative photomicrographs are shown (**B**). Each symbol represents an individual kidney. There were 7 PBS-treated WT mice, 11 PBS-treated caspase $1^{-/-}$ mice, 14 pristane-treated WT mice, and 23 pristane-treated caspase $1^{-/-}$ mice. Bars = 20 μm. **C** and **D,** Glomerular inflammation activity scores were determined on periodic acid–Schiff–stained, formalin-fixed kidney sections from WT or caspase $1^{-/-}$ mice exposed to PBS or pristane. Composite scores were averaged (**C**). Each symbol represents an individual kidney. Representative photomicrographs (**D**) demonstrate enlarged, hypercellular glomeruli due to mesangial and endocapillary inflammation in pristane-treated WT mice, but not in pristane-treated caspase $1^{-/-}$ mice. There were 6 PBS-treated WT mice, 8 PBS-treated caspase $1^{-/-}$ mice, 14 pristane-treated WT mice, and 19 pristane-treated caspase $1^{-/-}$ mice. Bars = 100 μm. **E,** Microalbumin-to-creatinine (microalb/Cr) ratios were determined in urine collected at the time of euthanasia. **F,** Levels of IL-18 in serum collected 5 months after PBS or pristane treatment were determined by enzyme-linked immunosorbent assay. In **E** and **F,** there were 7 PBS-treated WT mice, 11 PBS-treated caspase $1^{-/-}$ mice, 14 pristane-treated WT mice, and 23 pristane-treated caspase $1^{-/-}$ mice. **G,** Linear regression of the IL-18 concentration versus the renal activity score in pristane-treated WT mice (n = 12) is shown. Bars show the mean ± SEM. * = $P < 0.05$; ** = $P < 0.01$; *** = $P < 0.001$. IF = immunofluorescence (see Figure 1 for other definitions).

sure to pristane. However, following exposure to PBS or pristane, both BALB/c and C57BL/6 caspase $1^{-/-}$ mice displayed significant increases in endothelium-dependent vasorelaxation when compared to WT mice (Figure 3D). These results indicate that caspase 1 modulates the vasodilatory capacity of the endothelium, independent of lupus phenotype or mouse strain.

Caspase 1 is required for the development of immune complex glomerulonephritis in pristane-induced lupus. As expected, pristane exposure resulted in prominent immune complex deposition in the glomeruli of WT BALB/c mice. In contrast, caspase $1^{-/-}$ mice had significant decreases in glomerular immune complex deposition (Figures 4A and B). Furthermore, lack of caspase 1 protected BALB/c mice exposed to pristane from glomerular inflammation (Figures 4C and D). Decreases in immune complex deposition and renal inflammation in caspase $1^{-/-}$ mice correlated significantly with decreases in titers of anti-dsDNA, anti-RNP, and total IgG (not shown). While WT BALB/c mice showed a trend toward increased albuminuria following pristane exposure, caspase $1^{-/-}$ mice did not have similar increases after pristane exposure (Figure 4E). Similar patterns were found when examining total protein-to-creatinine ratios (not shown). Further, WT mice exposed to pristane, but not caspase $1^{-/-}$ mice exposed to pristane, showed a trend toward increased serum IL-18 levels, and the serum concentration of IL-18 correlated significantly with the severity of nephritis in WT mice exposed to pristane (Figures 4F and G). These results indicate that glomerular immune complex deposition and renal inflammation are hampered in the absence of

caspase 1 and that activation of IL-18 by caspase 1 may be an important step in nephritis induction in this model.

DISCUSSION

The development of lupus is considered to be the result of an aberrant interplay between innate and adaptive immune responses. Recently, it has been proposed that the inflammasome machinery is dysregulated in lupus systems secondary to type I IFN, aberrant cell death, and autoantibody-mediated effects (4,10–12,34). The results presented here identify novel roles for caspase 1, the central enzyme of the inflammasome, in the pristane-induced model of lupus. Indeed, the absence of caspase 1 abrogated known hallmarks of murine and human SLE, including autoantibody development, type I IFN signatures, and renal inflammation.

There are several likely mechanisms by which caspase 1 modulates lupus development. Serum levels of IL-18 are elevated in SLE patients and have been correlated with disease severity and lupus nephritis (17,35,36), and in the MRL-Fas^{lpr} lupus model, a role has been proposed for IL-18 in nephritis and skin disease (37). IL-18 regulates IFNγ production (38), and this may further modulate SLE development as IFNγ is required for disease pathology (39). Up-regulation of IL-1β and IL-18 transcripts in response to pristane was not observed in caspase $1^{-/-}$ mice, suggesting that pristane may require caspase 1–dependent pathways to induce these cytokines. Additionally, the severity of nephritis correlated significantly with serum levels of IL-18 in these mice, suggesting that caspase 1 activation of IL-18 may play a pathogenic role in nephritis induction.

Despite the profound effect on lupus development, lack of caspase 1 did not affect peritoneal inflammatory responses to pristane. Indeed, enhanced neutrophil recruitment was observed in the peritoneal cavity of pristane-treated caspase $1^{-/-}$ mice. Previously, the recruitment of neutrophils following pristane exposure was shown to be dependent on IL-1α–mediated up-regulation of CXCL5 (40). This cytokine is secreted in a caspase 1–dependent manner and expressed on the cell surface in a caspase 1–independent manner. Cell surface IL-1α is increased following inhibition of caspase 1 (41); thus, the paradoxical increase in neutrophils seen in caspase $1^{-/-}$ mice may be secondary to increased expression of surface IL-1α. Additionally, increased surface IL-1α in the absence of caspase 1 may explain the enhanced basal CXCL5 expression seen in caspase $1^{-/-}$ mice.

The induction of accelerated cell death and aberrant uptake of apoptotic debris has been postulated as a mechanism for lupus induction (27). Thus, lack of caspase 1 may be protective against inflammatory responses initiated by apoptotic debris. Furthermore, in addition to its role as activator of IL-1β and IL-18, caspase 1 is also required for induction of inflammatory cell death, which is also known as pyroptosis. While traditionally activated by intracellular bacterial infection, caspase 1–dependent cell death may also be a relevant physiologic cell death pathway (for review, see ref. 42). Importantly, the phagocytosis of pyroptotic debris may occur through similar "eat me" signals employed by apoptotic cells (28). We hypothesize that aberrant clearance of pyroptotic debris may also contribute to SLE pathogenesis. Our data show decreased annexin V staining of inflammatory cells following pristane exposure in caspase $1^{-/-}$ mice, and annexin V staining detects both apoptotic and pyroptotic debris (28). As such, down-regulation of inflammatory cell death following pristane exposure may decrease autoantigen externalization, limit aberrant autoantibody formation, and decrease type I IFN synthesis. Future studies should further test this hypothesis.

Caspase $1^{-/-}$ mice exposed to pristane lack significant autoantibody development. Because autoreactive B cells are activated by RNP autoantigens (43), the abrogation of cell death pathways in caspase $1^{-/-}$ mice likely decreases B cell activation. Further, the profound lack of chronic type I IFN up-regulation in caspase $1^{-/-}$ mice may have negative effects on B cells, as type I IFN production is an important mediator of B cell activation and class switching (44). Decreased IL-6 production in caspase $1^{-/-}$ mice may also contribute to lower autoantibody titers, given that this cytokine has been reported to synergize with type I IFN responses to induce maturation of B cells into highly functional IgG-secreting plasma cells (45), as well as to promote many other proinflammatory responses.

The role of caspase 1 may relate not only to autoantibody development in response to pristane but also to downstream responses to immune complexes. Recently, activation of the inflammasome via U1 small nuclear RNP–anti-RNP complexes through TLR-7 stimulation was described in human monocytes (11), and similar responses occur in response to dsDNA–anti-dsDNA antibody complexes (12). Further, caspase 1 activation is enhanced in SLE macrophages in response to NETs (10). The associated cytokine generation further enhances inflammatory responses and NET forma-

tion, which can result in circulating immune complexes capable of stimulating PDC activation and type I IFN production (46). Thus, caspase 1 likely plays important roles in both autoantibody generation and inflammatory responses downstream of immune complexes.

With regard to the role of caspase 1 in SLE-associated CV disease, lack of caspase 1 improved EPC differentiation in the pristane-induced model of lupus. This supports our previous observations that inhibition of caspase 1 provides a vasculoprotective effect in human SLE (4). Others have demonstrated similar effects on atherosclerosis development in apolipoprotein E–null mice (30).

Endothelium-dependent vasorelaxation was increased in the absence of caspase 1, independently of mouse strain or lupus phenotype. The mechanisms behind this enhanced relaxation in caspase $1^{-/-}$ mice may be secondary to a combination of decreased endothelial damage and enhanced vascular repair. The inflammasome plays a role in response to cholesterol crystals and generation of inflammatory responses in plaque (29). Without active caspase 1, the negative effects of vascular inflammation on the endothelium are likely dampened. Further, type I IFNs and IL-18 have negative effects on vascular repair (2,4,47). As caspase $1^{-/-}$ mice have repressed type I IFN responses and do not activate IL-18, this may lead to improved EPC differentiation and endothelial function. Additional studies are nevertheless required to further define how caspase 1 inhibition improves vascular function in murine and human systems (47–49).

This study has some limitations. The experimental design addresses the role of caspase 1 in pristane-induced lupus, but it does not provide information on specific activation of the inflammasome in this model. Additionally, recent observations on the caspase $1^{-/-}$ mouse have revealed that it contains a nonfunctional caspase 11 gene (50). While not required for classic inflammasome activation, caspase 11 may be important for pathogen-induced inflammasome assembly and in mediating pyroptosis in response to infection (50). Further experiments should be performed to address the role of caspase 11 specifically in the pristane-induced model of lupus.

In summary, we have demonstrated a role of caspase 1 in the development of murine lupus as its absence is characterized by significant down-modulation of autoantibody synthesis, type I IFN responses, glomerulonephritis, and vascular dysfunction. These results indicate the need to further explore the inflammasome as a putative therapeutic target in this disease.

AUTHOR CONTRIBUTIONS

All authors were involved in drafting the article or revising it critically for important intellectual content, and all authors approved the final version to be published. Drs. Kahlenberg and Kaplan had full access to all of the data in the study and take responsibility for the integrity of the data and the accuracy of the data analysis.

Study conception and design. Kahlenberg, Yalavarthi, Tsuji, Kaplan.
Acquisition of data. Kahlenberg, Yalavarthi, Zhao, Hodgin, Reed.
Analysis and interpretation of data. Kahlenberg, Yalavarthi, Zhao, Hodgin, Kaplan.

REFERENCES

1. Ward MM. Premature morbidity from cardiovascular and cerebrovascular diseases in women with systemic lupus erythematosus. Arthritis Rheum 1999;42:338–46.
2. Denny MF, Thacker S, Mehta H, Somers EC, Dodick T, Barrat FJ, et al. Interferon-α promotes abnormal vasculogenesis in lupus: a potential pathway for premature atherosclerosis. Blood 2007;110:2907–15.
3. Kirou K, Lee C, George S, Louca K, Peterson MG, Crow MK. Activation of the interferon-α pathway identifies a subgroup of systemic lupus erythematosus patients with distinct serologic features and active disease. Arthritis Rheum 2005;52:1491–503.
4. Kahlenberg JM, Thacker SG, Berthier CC, Cohen CD, Kretzler M, Kaplan MJ. Inflammasome activation of IL-18 results in endothelial progenitor cell dysfunction in systemic lupus erythematosus. J Immunol 2011;187:6143–56.
5. Reeves WH, Lee PY, Weinstein JS, Satoh M, Lu L. Induction of autoimmunity by pristane and other naturally occurring hydrocarbons. Trends Immunol 2009;30:455–64.
6. Lee PY, Kumagai Y, Li Y, Takeuchi O, Yoshida H, Weinstein J, et al. TLR7-dependent and FcγR-independent production of type I interferon in experimental mouse lupus. J Exp Med 2008;205:2995–3006.
7. Thibault D, Graham K, Lee L, Balboni I, Hertzog P, Utz P. Type I interferon receptor controls B-cell expression of nucleic acid-sensing Toll-like receptors and autoantibody production in a murine model of lupus. Arthritis Res Ther 2009;11:R112.
8. Lee PY, Li Y, Kumagai Y, Xu Y, Weinstein JS, Kellner ES, et al. Type I interferon modulates monocyte recruitment and maturation in chronic inflammation. Am J Pathol 2009;175:2023–33.
9. Lamkanfi M, Dixit VM. Inflammasomes and their roles in health and disease. Annu Rev Cell Dev Biol 2012;28:137–61.
10. Kahlenberg JM, Carmona-Rivera C, Smith CK, Kaplan MJ. Neutrophil extracellular trap–associated protein activation of the NLRP3 inflammasome is enhanced in lupus macrophages. J Immunol 2013;190:1217–26.
11. Shin MS, Kang Y, Lee N, Kim SH, Kang KS, Lazova R, et al. U1-small nuclear ribonucleoprotein activates the NLRP3 inflammasome in human monocytes. J Immunol 2012;188:4769–75.
12. Shin MS, Kang Y, Lee N, Wahl ER, Kim SH, Kang KS, et al. Self double-stranded (ds)DNA induces IL-1β production from human monocytes by activating NLRP3 inflammasome in the presence of anti-dsDNA antibodies. J Immunol 2013;190:1407–15.
13. Zhao W, Thacker SG, Hodgin JB, Zhang H, Wang JH, Park JL, et al. The peroxisome proliferator-activated receptor γ agonist pioglitazone improves cardiometabolic risk and renal inflammation in murine lupus. J Immunol 2009;183:2729–40.
14. Boxio R, Bossenmeyer-Pourie C, Steinckwich N, Dournon C, Nusse O. Mouse bone marrow contains large numbers of functionally competent neutrophils. J Leukoc Biol 2004;75:604–11.
15. Villanueva E, Yalavarthi S, Berthier CC, Hodgin JB, Khandpur R, Lin AM, et al. Netting neutrophils induce endothelial damage, infiltrate tissues, and expose immunostimulatory molecules in systemic lupus erythematosus. J Immunol 2011;187:538–52.

16. Liu X, Bao C, Hu D. Elevated interleukin-18 and skewed Th1:Th2 immune response in lupus nephritis. Rheumatol Int 2012;32: 223–9.
17. Tucci M, Quatraro C, Lombardi L, Pellegrino C, Dammacco F, Silvestris F. Glomerular accumulation of plasmacytoid dendritic cells in active lupus nephritis: role of interleukin-18. Arthritis Rheum 2008;58:251–62.
18. Herman S, Kny A, Schorn C, Pfatschbacher J, Niederreiter B, Herrmann M, et al. Cell death and cytokine production induced by autoimmunogenic hydrocarbon oils. Autoimmunity 2012;45: 602–11.
19. Yang L, Feng D, Bi X, Stone RC, Barnes BJ. Monocytes from irf5$^{-/-}$ mice have an intrinsic defect in their response to pristane-induced lupus. J Immunol 2012;189:3741–50.
20. Xu Y, Lee PY, Li Y, Liu C, Zhuang H, Han S, et al. Pleiotropic IFN-dependent and -independent effects of IRF5 on the pathogenesis of experimental lupus. J Immunol 2012;188:4113–21.
21. Weinstein JS, Delano MJ, Xu Y, Kelly-Scumpia KM, Nacionales DC, Li Y, et al. Maintenance of anti-Sm/RNP autoantibody production by plasma cells residing in ectopic lymphoid tissue and bone marrow memory B cells. J Immunol 2013;190:3916–27.
22. Feng D, Yang L, Bi X, Stone RC, Patel P, Barnes BJ. Irf5-deficient mice are protected from pristane-induced lupus via increased Th2 cytokines and altered IgG class switching. Eur J Immunol 2012; 42:1477–87.
23. Weckerle CE, Franek BS, Kelly JA, Kumabe M, Mikolaitis RA, Green SL, et al. Network analysis of associations between serum interferon-α activity, autoantibodies, and clinical features in systemic lupus erythematosus. Arthritis Rheum 2011;63:1044–53.
24. Agrawal H, Jacob N, Carreras E, Bajana S, Putterman C, Turner S, et al. Deficiency of type I IFN receptor in lupus-prone New Zealand mixed 2328 mice decreases dendritic cell numbers and activation and protects from disease. J Immunol 2009;183:6021–9.
25. Savarese E, Steinberg C, Pawar RD, Reindl W, Akira S, Anders HJ, et al. Requirement of Toll-like receptor 7 for pristane-induced production of autoantibodies and development of murine lupus nephritis. Arthritis Rheum 2008;58:1107–15.
26. Lee PY, Weinstein JS, Nacionales DC, Scumpia PO, Li Y, Butfiloski E, et al. A novel type I IFN-producing cell subset in murine lupus. J Immunol 2008;180:5101–8.
27. White S, Rosen A. Apoptosis in systemic lupus erythematosus. Curr Opin Rheumatol 2003;15:557–62.
28. Wang Q, Imamura R, Motani K, Kushiyama H, Nagata S, Suda T. Pyroptotic cells externalize eat-me and release find-me signals and are efficiently engulfed by macrophages. Int Immunol 2013;25: 363–72.
29. Duewell P, Kono H, Rayner KJ, Sirois CM, Vladimer G, Bauernfeind FG, et al. NLRP3 inflammasomes are required for atherogenesis and activated by cholesterol crystals. Nature 2010;464: 1357–61.
30. Gage J, Hasu M, Thabet M, Whitman SC. Caspase-1 deficiency decreases atherosclerosis in apolipoprotein E-null mice. Can J Cardiol 2012;28:222–9.
31. Briasoulis A, Tousoulis D, Antoniades C, Papageorgiou N, Stefanadis C. The role of endothelial progenitor cells in vascular repair after arterial injury and atherosclerotic plaque development. Cardiovasc Ther 2011;29:125–39.
32. Vasa M, Fichtlscherer S, Aicher A, Adler K, Urbich C, Martin H, et al. Number and migratory activity of circulating endothelial progenitor cells inversely correlate with risk factors for coronary artery disease. Circ Res 2001;89:E1–7.
33. Thacker SG, Duquaine D, Park J, Kaplan MJ. Lupus-prone New Zealand Black/New Zealand White F1 mice display endothelial dysfunction and abnormal phenotype and function of endothelial progenitor cells. Lupus 2010;19:288–99.
34. Zhang W, Cai Y, Xu W, Yin Z, Gao X, Xiong S. AIM2 facilitates the apoptotic DNA-induced systemic lupus erythematosus via arbitrating macrophage functional maturation. J Clin Immunol 2013;33:925–37.
35. Hu D, Liu X, Chen S, Bao C. Expressions of IL-18 and its binding protein in peripheral blood leukocytes and kidney tissues of lupus nephritis patients. Clin Rheumatol 2010;29:717–21.
36. Calvani N, Richards HB, Tucci M, Pannarale G, Silvestris F. Up-regulation of IL-18 and predominance of a Th1 immune response is a hallmark of lupus nephritis. Clin Exp Immunol 2004;138:171–8.
37. Kinoshita K, Yamagata T, Nozaki Y, Sugiyama M, Ikoma S, Funauchi M, et al. Blockade of IL-18 receptor signaling delays the onset of autoimmune disease in MRL-Faslpr mice. J Immunol 2004;173:5312–8.
38. Lee JK, Kim SH, Lewis EC, Azam T, Reznikov LL, Dinarello CA. Differences in signaling pathways by IL-1β and IL-18. Proc Natl Acad Sci U S A 2004;101:8815–20.
39. Richards HB, Satoh M, Jennette JC, Croker BP, Yoshida H, Reeves WH. Interferon-γ is required for lupus nephritis in mice treated with the hydrocarbon oil pristane. Kidney Int 2001;60: 2173–80.
40. Lee PY, Kumagai Y, Xu Y, Li Y, Barker T, Liu C, et al. IL-1α modulates neutrophil recruitment in chronic inflammation induced by hydrocarbon oil. J Immunol 2011;186:1747–54.
41. Fettelschoss A, Kistowska M, LeibundGut-Landmann S, Beer HD, Johansen P, Senti G, et al. Inflammasome activation and IL-1β target IL-1α for secretion as opposed to surface expression. Proc Natl Acad Sci U S A 2011;108:18055–60.
42. Denes A, Lopez-Castejon G, Brough D. Caspase-1: is IL-1 just the tip of the ICEberg? Cell Death Dis 2012;3:e338.
43. Green NM, Moody KS, Debatis M, Marshak-Rothstein A. Activation of autoreactive B cells by endogenous TLR7 and TLR3 RNA ligands. J Biol Chem 2012;287:39789–99.
44. Swanson CL, Wilson TJ, Strauch P, Colonna M, Pelanda R, Torres RM. Type I IFN enhances follicular B cell contribution to the T cell–independent antibody response. J Exp Med 2010;207: 1485–500.
45. Jego G, Palucka AK, Blanck JP, Chalouni C, Pascual V, Banchereau J. Plasmacytoid dendritic cells induce plasma cell differentiation through type I interferon and interleukin 6. Immunity 2003;19:225–34.
46. Lande R, Ganguly D, Facchinetti V, Frasca L, Conrad C, Gregorio J, et al. Neutrophils activate plasmacytoid dendritic cells by releasing self-DNA-peptide complexes in systemic lupus erythematosus. Sci Transl Med 2011;3:73ra19.
47. Thacker SG, Zhao W, Smith CK, Luo W, Wang H, Vivekanandan-Giri A, et al. Type I interferons modulate vascular function, repair, thrombosis, and plaque progression in murine models of lupus and atherosclerosis. Arthritis Rheum 2012;64:2975–85.
48. Kahlenberg JM, Kaplan MJ. The interplay of inflammation and cardiovascular disease in systemic lupus erythematosus. Arthritis Res Ther 2011;13:203.
49. Niessner A, Weyand CM. Dendritic cells in atherosclerotic disease. Clin Immunol 2010;134:25–32.
50. Kayagaki N, Warming S, Lamkanfi M, Walle LV, Louie S, Dong J, et al. Non-canonical inflammasome activation targets caspase-11. Nature 2011;479:117–21.